10. Mamtani, M. A., Karanth, R. V., Merh, S. S. and Greiling, R. O., *Gondwana Res.*, 2000, **3**, 175–187.
11. Mamtani, M. A., Merh, S. S., Karanth, R. V. and Greiling, R. O., *J. Asia Earth Sci.*, 2001, **19**, 195–205.
12. https://sentinel.esa.int/web/sentinel/user-guides/sentinel-2-msi
13. Mukherjee, S., *Atlas of Shear Zone Structures in Meso-Scale*, Springer Geology, Berlin, Germany, 2014, pp. 1–124; ISBN 978-3-319-0088-6.
14. Mukherjee, S., *Atlas of Structural Geology*, Elsevier, Amsterdam, The Netherlands, 2015.
15. Joshi, A., Limaye, M. A. and Deota, B. S., *Int. J. Earth Sci.*, 2018, **108**(1), 183–186.
16. Lister, G. S. and Snoke, A. W., *J. Struct. Geol.*, 1984, **6**(6), 617–638.
17. Passchier, C. W., *J. Struct. Geol.*, 2001, **23**(6), 951–962.
18. Grasemann, B., Stüwe, K. and Vannay, J. C., *J. Struct. Geol.*, 2003, **25**(1), 19–34.
19. Mukherjee, S. and Koyi, H. A., *Geol. Mag.*, 2009, **146**, 517–526.
20. Mukherjee, S., *YES Bull.*, 2011, **1**, 21–29.
21. Biswas, A. and Roy, P., *Int. J. Earth Sci.*, 2018, **107**, 167–168.
22. Exner, U., Mancktelow, N. S. and Grasemann, B., *J. Struct. Geol.*, 2004, **26**(12), 2191–2201.

ACKNOWLEDGEMENTS. We thank Dr S. Mukherjee (Department of Earth Sciences, IIT Bombay) for useful comments and suggestions. We also thank Prof. M. Mamtani (Department of Geology and Geophysics, IIT Kharagpur) for his comments on the initial version of this paper.

Received 21 April 2020; revised accepted 1 July 2020

PRIYOM ROY[1,*]
ANKITA BISWAS[2]

[1]*National Remote Sensing Centre, Indian Space Research Organisation,*
[2]*Geological Survey of India, Hyderabad 500 068, India*
**For correspondence.*
e-mail: roy.priyom@gmail.com

Uranium and associated polymetallic mineralization in Palaeoproterozoic Khetabari Formation of Bomdila Group, Laggi Gamlin area, West Siang district, Arunachal Pradesh, India

Palaeoproterozoic Khetabari Formation of Bomdila Group in Arunachal Pradesh, India is an N–S to NE–SW trending volcano-sedimentary sequence. It stratigraphically overlies the Se La Group and is exposed in the western limb of Siang antiform (Figure 1 *a*). The Khetabari Formation comprises calc–silicate rocks/marble, carbonaceous phyllite, magnetite quartzite, quartzite/schistose quartzite and mica schist (Figure 1 *b* and *c*) with some concordant and discordant basic intrusions. It is thrusted over the Palaeoproterozoic Tenga Formation in the eastern margin[1]. Intrusive Ziro granite gneiss (1536–1914 Ma) is exposed along its western margin[2]. Multiple episodes of deformation have affected the Khetabari Formation. F1 folds well-preserved in massive and schistose quartzites, show tight to isoclinal, reclined to recumbent geometry and their axial planes generally show N–S to NNE–SSW strike. The most pervasive planar fabric S1 is developed parallel to the axial plane of the F1 folds, and is predominantly parallel to the S0 plane. The F2 folds have coaxially refolded the axial planes of F1 folds giving rise to type-III interference patterns. Crenulation cleavage (S2) is related to F2 folding. Steeply plunging, inclined, open folds of the third generation superposed on earlier folds have N–S axial planes. N–S to NNE–SSW trending fault has given rise to fault breccia. Sigmoidal magnetite grains indicate sinistral shearing. In the shear zones, elongated quartz grains and S–C fabrics are noted. These structures have played a vital role in the circulation of mineralizing fluids in the Khetabari Formation, and have served as locales for uranium and associated polymetallic mineralization (Figure 2 *a* and *b*).

Exploration efforts over the last few decades in Arunachal Pradesh by the Atomic Minerals Directorate for Exploration and Research, Shillong have resulted in locating several uranium and associated polymetallic occurrences in the Khetabari Formation. Sie Rimi-Noko-Lete Nala[3,4], Gamkak-Tapeyor[5] and Kau Nala[6] are a few examples. They demonstrate the importance of structurally controlled uranium and associated polymetallic mineralization in the Khetabari Formation. Subsurface exploration at Noko Nala–Kardo–Badak area has established subsurface continuity of uranium mineralization in magnetite–calcite schist over a strike length of 1200 m with grade up to 0.036 %eU_3O_8 and thickness up to 8.1 m (ref. 4).

Here we provide details of recently located uranium and associated sulphide mineralization in a breccia zone (Laggi Gamlin-1; LGM-1) and in sheared magnetite quartzite (Laggi Gamlin-2; LGM-2) at Laggi Gamlin, West Siang district, Arunachal Pradesh (Figure 1).

The uranium mineralization of LGM-1 is hosted by breccia and is located in the first-order creek section about 900 m SSW of Laggi Gamlin village. The 1–10 m wide mineralization zone here is traced along the N–S strike over a length of 150 m. The strike coincides with the axial plane strike of F3 folds in the area. The breccia consists of few millimetres to more than 5 cm-sized calcite clasts cemented by ferruginous matter (Figure 2 *a*). The study reveals that ferruginous cement is radioactive. Thirteen samples of ferruginous breccia have assayed 0.009–0.027 (av. 0.012) %U_3O_8 and <0.005% ThO_2.

Petromineralogical study shows that breccia has developed from precursor calc–silicate rock/marble. It has angular clasts of calcitic marble which are cemented by a matrix composed of magnetite, hematite, K-feldspar and quartz (Figure 3 *a*). Accessory minerals are pyrite, chalcopyrite and rutile. Uranium occurs in the adsorbed state in magnetite and hematite in the matrix/cement of the brecciated marble.

The LGM-2 uranium mineralization is in sheared magnetite quartzite. Uranium

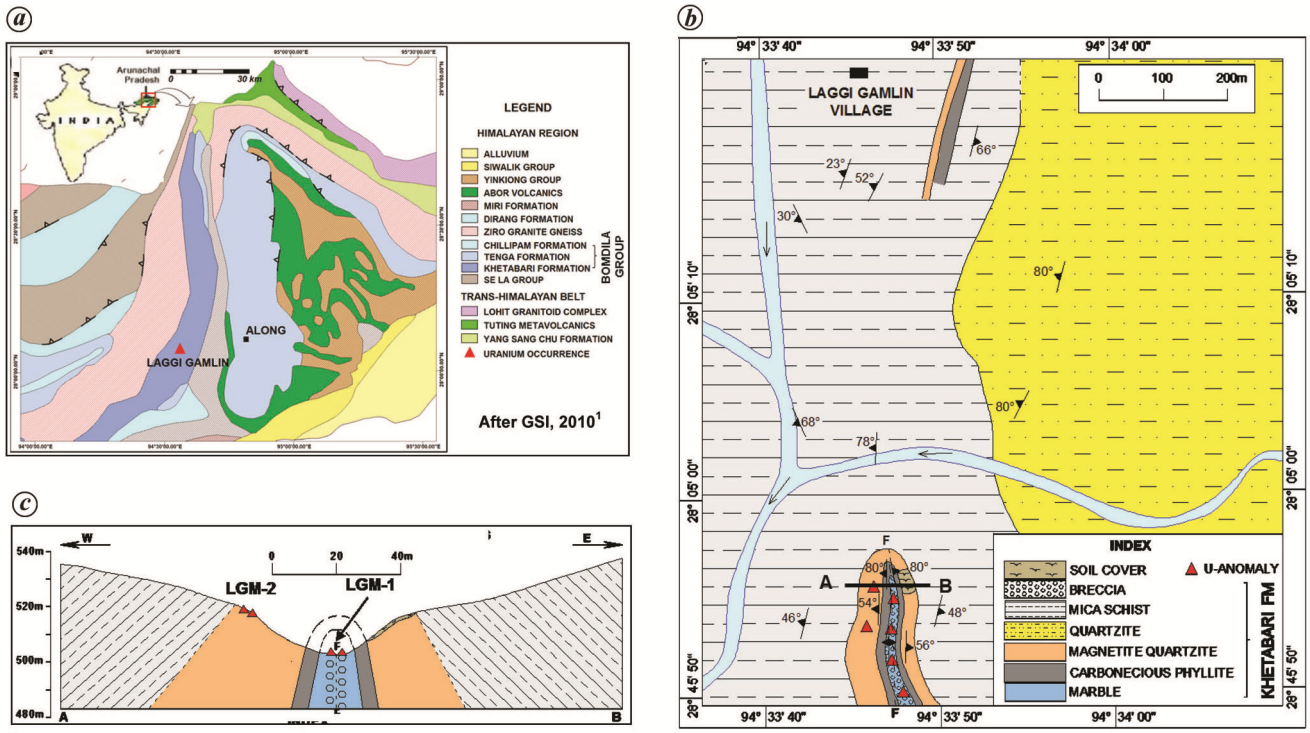

Figure 1. ***a***, Geological map and section showing location of Laggi Gamlin area, West Siang district, Arunachal Pradesh, India in the N–S to NE–SW trending Khetabari Formation of Bomdila Group in the western limb of Siang antiform. ***b***, Geological map of Laggi Gamlin, West Siang district, Arunachal Pradesh with section line A–B. ***c***, Geological section along A–B (index is same as in *b*).

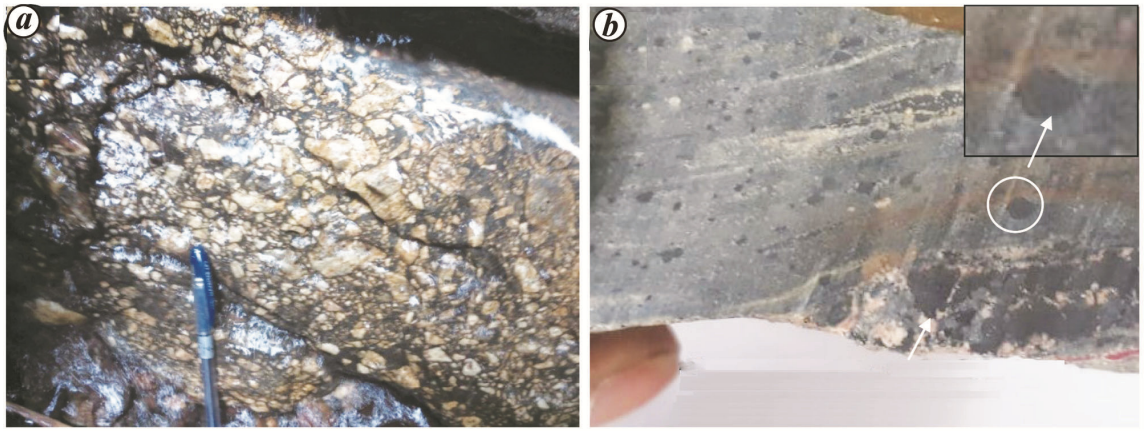

Figure 2. Field photographs of Laggi Gamlin area showing (***a***) uraniferous brecciated marble of Laggi Gamlin-1 uranium mineralization, and (***b***) sheared magnetite grain and uraniferous magnetite-bearing quartzofeldspathic vein in sheared magnetite quartzite of Laggi Gamlin-2 uranium mineralization.

mineralization is observed in a 60 m × 4 m area which is located about 20 m NW of LGM-1. The host rock magnetite quartzite is folded into a N–S antiform with limbs dipping about 50° westerly and easterly. Magnetite quartzite consists of quartz grains set in siliceous and ferruginous cement. It shows intensive shearing related to F3 deformation episode. The shearing is represented by sigmoidal magnetite grains (Figure 2 *b*), elongated quartz grains, S–C fabric and extensive development of micaceous minerals. Magnetite, tourmaline, chlorite and quartzo-feldspathic veins are emplaced along the shear planes. The emplacement of magnetite-bearing quartzo-feldspathic veins has played a major role in uranium mineralization, because uranium has precipitated along such veins as indicated by the chromogram test. Grab sample (n = 09) of sheared magnetite quartzite have been radiometrically assayed 0.013–0.390 %U_3O_8 (av. 0.154%) and <0.010 %ThO_2.

Sheared magnetite quartzite dominantly consists of quartz, magnetite and muscovite with few flakes of biotite. In addition, pyrite, monazite, zircon and apatite occur as accessory minerals. The S-planes are well developed by layering of muscovite flakes (Figure 3 *b*). Microscopic evidences of shearing are

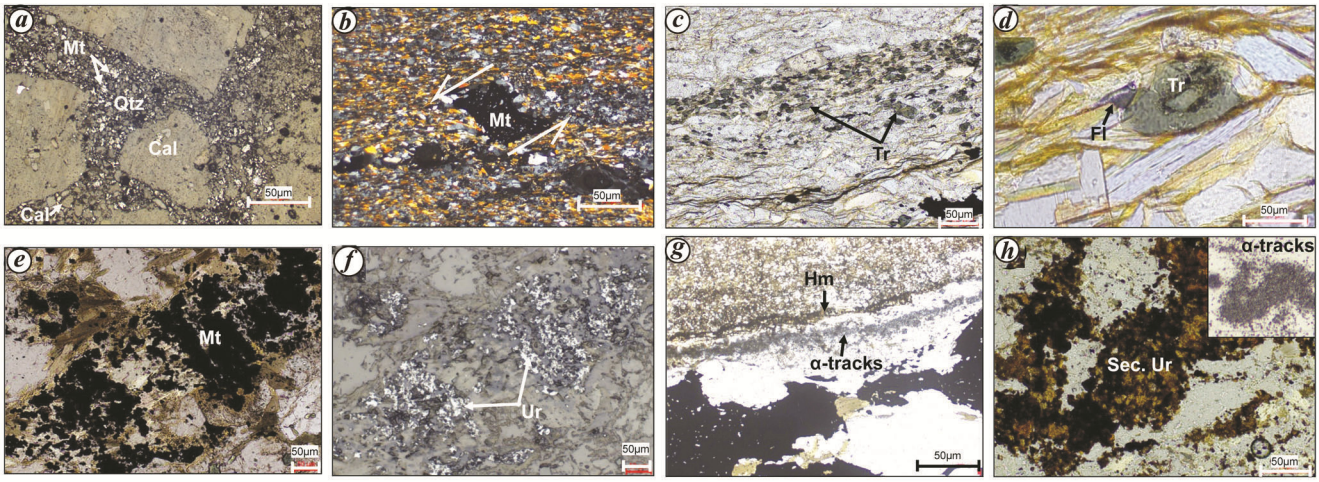

Figure 3. Photomicrographs of Laggi Gamlin area showing (***a***) angular clast of calcite (Cal) bounded by matrix and cement of magnetite (Mt), calcite and quartz (Qtz) in ferruginous breccia, (***b***) sheared magnetite grain in quartzite showing sinistral sense of movement, (***c***) tourmaline (Tr)-bearing vein in sheared magnetite quartzite, (***d***) hydrothermal minerals tourmaline (Tr) and fluorite (Fl) in the ground mass, (***e***) magnetite-bearing vein in sheared magnetite quartzite, (***f***) ultrafine uraninite (Ur) within the magnetite, (***g***) adsorbed uranium corresponding to hematite (Hm) represented by dense α-tracks, and (***h***) secondary uranium (Sec. Ur) minerals and their α-tracks.

Table 1. Radio elemental distribution of different litho units of the Khetabari Formation and Ziro Granite Gneiss

Formation	Rock	U_3O_8 (ppm) (based on Ra eq data)	ThO_2 (ppm)
Ziro granite gneiss	Granite gneiss (n = 8)	5–45 (av. 16)	5–135 (av. 71)
Khetabari Formation	Mica schist (n = 23)	2–18 (av. 5)	6–40 (av. 27)
	Quartzite (n = 29)	2–8 (av. 3)	5–31 (av. 12)
	Magnetite quartzite (n = 19)	2–74 (av. 27)	2–24 (av. 9)
	Carbonaceous phyllite (n = 13)	2–38 (av. 13)	17–43 (av. 26)
	Calc-silicate/marble (n = 5)	2 (av. 2)	2–12 (av. 5)

represented by sigmoidal poikiloclastic magnetite grains, S–C fabric and mica fishes. Magnetite, tourmaline (Figure 3 *c* and *d*), fluorite (Figure 3 *d*), chlorite and quartzo-feldspathic veins are evidences of subsequent hydrothermal activity. Uraninite is the main uranium-bearing ore mineral identified in sheared magnetite quartzite and is closely associated with hydrothermal magnetite-bearing quartzo-feldspathic veins (Figure 3 *e* and *f*). Hematite has developed along the boundary of these veins. Adsorbed uranium associated with hematite shows linear, dense α-tracks in the cellulose nitrate (CN) film (Figure 3 *g*). Secondary uranium minerals show fluorescence. Under the microscope, secondary uranium minerals occur as bright-coloured and show dense α-tracks in the CN film (Figure 3 *h*).

Uraninite is confirmed by X-ray diffraction. Other radioactive minerals like schoepite, monazite, xenotime and zircon have also been identified. Unit-cell dimension of uraninite (a_0) = 5.4660 ± 0.0006 Å and unit cell volume (V) = 163.316 Å^3 correspond to that found in hydrothermal vein-type deposits[7].

Geochemically, brecciated marble (n = 13) is characterized by higher values of Fe_2O_3 (15.2–54.33%), CaO (0.27–43.09%), TiO_2 (0.10–5.02%), and low values of SiO_2 (8.35–23.28%), Al_2O_3 (1.46–8.26%), MgO (0.26–0.94%), MnO (<0.01–0.14%), Na_2O (<0.01–2.09%), K_2O (0.37–0.84%) and P_2O_5 (<0.01–0.11%). Higher Fe_2O_3 content in the rock is due to the presence of magnetite and hematite in the matrix/cement, and higher CaO content is mainly due to calcite clasts. Higher TiO_2 content is attributed to the presence of rutile. Significant positive correlation (r = +0.85) between U_3O_8 and Fe_2O_3 confirms the role of iron in uranium mineralization. The concentration of associated trace elements in ferruginous breccia is 2216–10100 ppm Cu, 50–70 ppm Co, 22–600 ppm Ni, 35–76 ppm Zn, <10–90 ppm Mo, 150–800 ppb Au and 1899–5003 ppm ∑REE. They justify the polymetallic nature of mineralization.

Sheared magnetite quartzite (n = 9) has higher Fe_2O_3 (6.99–41.54%), Al_2O_3 (10.47–17.98%), K_2O (2.08–6.00%), and low to moderate SiO_2 (37.40–69.41%), Na_2O (<0.01–3.70%), TiO_2 (0.34–0.72%), MgO (0.15–3.71%), MnO (<0.01–0.64%), CaO (<0.01–3.7%) and P_2O_5 (<0.01–0.51%). Higher Fe_2O_3 (t) content in magnetite quartzite is due to the presence of detrital magnetite grains and magnetite veins. Higher K_2O and Al_2O_3 are due to muscovite, biotite and K-feldspar. Trace elements in magnetite quartzite (n = 9) are 8–23 ppm Cu, 48–52 ppm Co, <10–25 ppm Ni, 15–35 ppm Zn, <10–18 ppm Mo and 234–1479 ppm ∑REE. Such trace elemental association indicates significant role of hydrothermal fluid activity in bringing about uranium and rare earth mineralization hosted in the sheared magnetite quartzite. The intrinsic uranium content of non-mineralized magnetite quartzite (2–74 ppm, av.

27 ppm, $n = 19$) is higher than other litho-units of the Khetabari Formation (Table 1). This suggests that uranium might have been derived from the fertile Se La Group granitoids (12–60 ppm)[5].

Uranium mineralization in the Khetabari Formation involves two distinct processes: (i) syngenetic and (ii) epigenetic. Non-mineralized magnetite quartzite shows uranium abundance in the range 2–74 ppm (Table 1). Such high values are unusual, and may be due to derivation of uranium from fertile granite gneiss provenance belonging to the Se La Group. The fertile gneisses of Se La Group have high abundances of uranium ranging from 12 to 60 ppm[5]. Iron associated with magnetite quartzite could help in the precipitation of uranium from sea water during its deposition. The epigenetic hydrothermal process is evidenced by uraniferous magnetite-bearing quartzofeldspathic veins (Figure 2 *a*). The epigenetic hydrothermal mineralization has played a vital role in enrichment of uranium. The Ziro granite with 5–45 ppm, av. 16 ppm uranium content intruding the Khetabari Formation might have facilitated enrichment of uranium in the Formation. Fractures/faults/shear planes (Figure 3 *e* and *f*) acted as conduits and locales for uranium precipitation, as evident from vein-type uranium mineralization. Uranium is precipitated in the ferruginous breccia and sheared magnetite quartzite under the influence of reducing agents like sulphide and iron oxide.

The geological setting, presence of higher intrinsic uranium content in country rocks, prevailing fractures, faults and shears as conduits, hydrothermal alterations and favourable geochemical signatures suggest that Laggi Gamlin and adjoining areas are potential targets for multi-metal (U–Fe–Cu–Au–REEs)-type uranium mineralization. This finding opens up a novel target area for uranium exploration in the Khetabari Formation.

1. GSI, Geology and Mineral Resourse of Arunachal Pradesh. Misc. Publ. No. 30, Part IV, V1 (i), GSI, NER, Shillong, 2010, p. 54.
2. Dikshitulu, G. R., Pandey, B. K., Krishna, V. and Dhanaraju, R., *J. Geol. Soc. India*, 1995, **45**, 51–56.
3. Basu, B., Sharma, M., Gupta, C. S., Thippeswamy, S., Jeyagopal, A. V., Joshi, G. B. and Mohanty, R., *Curr. Sci.*, 2015, **108**, 1216–1218.
4. Pravin Kumar, J., Goyal, N., Sharma, M., Dash, J. K., Jeyagopal, A. V. and Joshi, G. B., *EARFAM*, 2015, **25**, 169–174.
5. Bisht, B. S., Ali, M. A., Pande, A. K. and Pavanagaru, R., *J. Geol. Soc. India*, 2005, **66**, 185–202.
6. Jain, R. C., Bajpai, R. K. and Kumar, D., *J. At. Miner. Sci.*, 1996, **4**, 33–36.
7. Berman, R. M., *Am. Mineral.*, 1957, **42**, 705–731.

ACKNOWLEDGEMENTS. We thank the Officers and staff of the Physics, Chemistry and Petrology Laboratories, Atomic Minerals Directorate for Exploration and Research (AMD), North Eastern Region, Shillong, and X-ray fluorescence and X-ray diffraction laboratories, AMD, Hyderabad for analytical support.

Received 17 January 2020; revised accepted 2 July 2020

SANTU PATRA[1,*]
JITU GOGOI[1]
U. P. SHARMA[1]
RAHUL BANERJEE[1]
D. K. SINHA[2]

[1]*Atomic Minerals Directorate for Exploration and Research, Shillong 793 019, India*
[2]*Atomic Minerals Directorate for Exploration and Research, Hyderabad 500 016, India*
**For correspondence.*
e-mail: santupatra.amd@gov.in